# Templated Mesoporous Silica Colloids with Controlled Internal Structures

Weon-Sik Chae and Paul V. Braun*

*Department of Materials Science and Engineering, Frederick Seitz Materials Research Laboratory, and Beckman Institute, University of Illinois at Urbana-Champaign, Urbana, Illinois 61801*

*Received June 19, 2007. Revised Manuscript Received September 5, 2007*

Mesoporous silica colloids (MSCs) are synthesized in the cavities of a polymer-based inverse opal. The spherical cavities of the polymer inverse opal provide a highly defined complex three-dimensionally confining environment for the cooperative assembly of silica precursors and the associated triblock copolymer mesophase, which appears to be maintained in the final MSCs. The internal mesostructure of the MSCs is regulated by the diameter, surface chemistry, and connectivity of the cavities in the polymer inverse opal. The diameter of the MSCs is controlled by the diameter of the cavities in the polymer inverse opal. When formed in hydrophilic polymer inverse opals, simple MSCs exhibiting a circularly wound concentric mesostructure are formed. At intermediate surface energies, the mesostructure exhibits a pseudo-rhombohedral dodecahedral organization, and when the MSCs are formed in a hydrophobic polymer inverse opal, their mesostructure becomes disordered. The average number of interconnects between cavities of the polymer inverse opal could be modulated by intentionally ordering or disordering the silica colloidal crystal used to template the polymer inverse opal; increasing disorder decreased the average number of interconnects between cavities. With use of such templates, the effect of interconnects on the MSCs was determined.

## Introduction

Mesoporous materials have been extensively studied because of their distinctive characteristics including tailorable mesostructure, controllable pore size, and high specific surface area.[1] In bulk systems, the structure of mesoporous material varies according to the concentration of surfactant and inorganic precursor, the solvent, and temperature, as all these parameters modify the lyotropic mesophases responsible for the formation of the mesoporous material.[2] When the precursors to the mesostructured materials are introduced into a confined environment, additional factors including structural frustration, interfacial interactions, and confinement-induced entropy loss work can strongly modulate the structure of the mesophase.[3] Mesoporous films formed between two solid surfaces are a good example of a one-dimensionally confined system.[4] Mesoporous fibers synthesized inside of microcylindrical channels are interesting examples of two-dimensionally confined systems. Depending on the diameter of the microcylindrical templates, the confinement-induced mesoporous fibers can show internal morphologies including concentric circularly wound, concentric lamellar, single- and double-helical, inverted peapod, and simple straight mesochannels.[3,5] Such unique mesostructures are impossible to obtain in unconfined bulk lyotropic systems. If the mesoporous material has chemical, optical, or electrical functionalities,[6] these unique confinement-induced mesoporous structures may modulate the properties in useful and interesting ways for applications including molecular catalysis, molecular sensors, and drug delivery.[7] Although multiple studies have been explored on these one- and two-dimensionally confined mesoporous systems,[4−6,8] there are few controlled studies on mesoporous

* Corresponding author. Phone: 217-244-7293. Fax: 217-333-2736. E-mail: pbraun@uiuc.edu.

(1) (a) Beck, J. S.; Vartuli, J. C.; Roth, W. J.; Leonowicz, M. E.; Kresge, C. T.; Schmitt, K. D.; Chu, C. T.-W.; Olson, D. H.; Sheppard, E. W.; McCullen, S. B.; Higgins, J. B.; Schlenker, J. L. *J. Am. Chem. Soc*. **1992**, *114*, 10834. (b) Zhao, D.; Feng, J.; Huo, Q.; Melosh, N.; Fredrickson, G. H.; Chmelka, B. F.; Stucky, G. D. *Science* **1998**, *279*, 548. (c) Kruk, M.; Jaroniec, M.; Sakamoto, Y.; Terasaki, O.; Ryoo, R.; Ko, C. H. *J. Phys. Chem. B* **2000**, *104*, 292.

(2) Raman, N. K.; Anderson, M. T.; Brinker, C. J. *Chem. Mater*. **1996**, *8*, 1682.

(3) Wu, Y.; Cheng, G.; Katsov, K.; Sides, S. W.; Wang, J.; Tang, J.; Fredrickson, G. H.; Moskovits, M.; Stucky, G. D. *Nat. Mater*. **2004**, *3*, 816.

(4) Lambooy, P.; Russell, T. P.; Kellogg, G. J.; Mayes, A. M.; Gallagher, P. D.; Satija, S. K. *Phys. Rev. Lett*. **1994**, *72*, 2899.

(5) (a) Yang, Z.; Niu, Z.; Cao, X.; Yang, Z.; Lu, Y.; Hu, Z.; Han, C. C. *Angew. Chem., Int. Ed*. **2003**, *42*, 4201. (b) Lu, Q.; Gao, F.; Komarneni, S.; Mallouk, T. E. *J. Am. Chem. Soc*. **2004**, *126*, 8650. (c) Wang, D.; Kou, R.; Yang, Z.; He, J.; Yang, Z.; Lu, Y. *Chem. Commun*. **2005**, 166.

(6) (a) Chae, W.-S.; Lee, S.-W.; Im, S.-J.; Moon, S.-W.; Zin, W.-C.; Lee, J.-K.; Kim, Y.-R. *Chem. Commun*. **2004**, 2554. (b) Chae, W.-S.; Lee, S.-W.; An, M.-J.; Choi, K.-H.; Moon, S.-W.; Zin, W.-C.; Jung, J.-S.; Kim, Y.-R. *Chem. Mater*. **2005**, *17*, 5651. (c) Chae, W.-S.; Lee, S.-W.; Kim, Y.-R. *Chem. Mater*. **2005**, *17*, 3072. (d) Chae, W.-S.; An, M.-J.; Lee, S.-W.; Son, M.-S.; Yoo, K.-H.; Kim, Y.-R. *J. Phys. Chem. B* **2006**, *110*, 6447.

(7) (a) Kuśtrowski, P.; Chmielarz, L.; Dziembaj, R.; Cool, P.; Vansant, E. F. *J. Phys. Chem. A* **2005**, *109*, 330. (b) Bartl, M. H.; Puls, S. P.; Tang, J.; Lichtenegger, H. C.; Stucky, G. D. *Angew. Chem., Int. Ed*. **2004**, *43*, 3037. (c) Kim, J.; Lee, J. E.; Lee, J.; Yu, J. H.; Kim, B. C.; An, K.; Hwang, Y.; Shin, C.-H.; Park, J.-G.; Kim, J.; Hyeon, T. *J. Am. Chem. Soc*. **2006**, *128*, 688.

(8) (a) Yamaguchi, A.; Uejo, F.; Yoda, T.; Uchida, T.; Tanamura, Y.; Yamashita, T.; Teramae, N. *Nat. Mater*. **2004**, *3*, 337. (b) Yao, B.; Fleming, D.; Morris, M. A.; Lawrence, S. E. *Chem. Mater*. **2004**, *16*, 4851. (c) Liang, Z.; Susha, A. S. *Chem. Eur. J*. **2004**, *10*, 4910. (d) Platschek, B.; Petkov, N.; Bein, T. *Angew. Chem., Int. Ed*. **2006**, *45*, 1134.

10.1021/cm071642p CCC: $37.00 
Published on Web 10/12/2007

**Scheme 1. Outline of the Double-Replication Procedure Used To Synthesize the MSCs[a]**

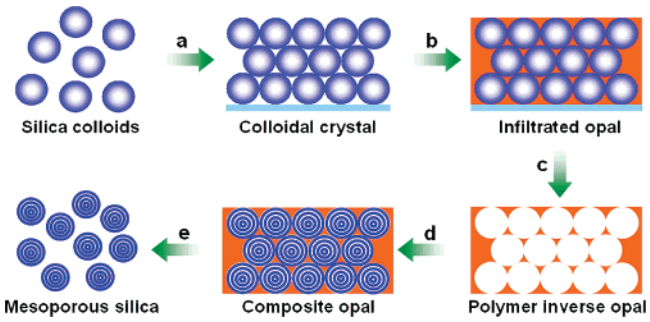


[a] (a) Self-assembly of colloidal silica particles on a glass slide, (b) polymer infiltration, (c) removal of the colloidal silica template and substrate with HF, (d) introduction of lyotropic mixture within the polymer inverse opal, and (e) calcination and sonication.

materials formed in three-dimensionally (3D) confining environments.[9]

In this study, we synthesize mesoporous silica colloids (MSCs) through a double-templating route. First, a colloidal silica opal is used to form a polymer inverse opal. Then, this polymer inverse opal is used as a reactor for the formation of mesoporous silica. The mesoporous silica precursor, a lyotropic mixture consisting of a triblock copolymer, silica precursors, and solvent, is introduced into the spherical void cavities of the polymer inverse opal through the interconnecting windows between adjacent void cavities. Each spherical void space in the polymer inverse opal provides a three-dimensionally confining environment for this lyotropic mesophase with a connectivity determined by the order in the initial silica opal. We observe that the internal mesostructure of the resulting MSCs can be controlled by the cavity surface chemistry and diameter, and by the number of interconnecting windows between the spherical cavities.

## Experimental Section

**Preparation of Polymer Inverse Opals.** A schematic for the synthesis of the MSCs is presented in Scheme 1. The initial step is the formation of the ordered or disordered polymer inverse opals, which serve as physical templates for the preparation of the MSCs; these inverse opals are formed via replication of a silica opal with a commercial polyurethane photopolymer (Norland Optical Adhesive; NOA 76), using a procedure adapted from the literature.[10] Silica microspheres, 178, 298, and 498 nm in diameter, with a narrow size distribution ($\delta$ < 2%) were synthesized using a microemulsion method and subsequent regrowth (Supporting Information, Figure S1).[11,12] Three to 5 $\mu$m thick silica opals were formed on glass slides using these microspheres dispersed in ethanol via controlled drying.[13] The NOA 76 prepolymer was infiltrated within the self-assembled colloidal silica opal at ~50 °C and subsequently polymerized under ultraviolet ($\lambda$ = 365 nm) irradiation (Blak-Ray B-100A Hg lamp, 100 W) for 1 h. After photopolymerization, the structure was placed overnight in aqueous HF (5 wt %), dissolving the substrate and the silica opal, resulting in free-standing polymer inverse opal films. (*Caution: HF is toxic.*) These films were washed multiple times with deionized water and dried overnight at ~70 °C. The resulting ordered polymer inverse opals were denoted PIO-S, PIO-M, and PIO-L, depending on the diameter of the initial silica microspheres, 178, 298, and 498 nm, respectively. The disordered polymer inverse opal template was fabricated using a disordered aggregate of silica microsphere (298 nm), applying the same polymer replication procedures described above. The disordered silica aggregate was formed by rapidly drying an ethanolic suspension of microspheres on a hot glass substrate (70−80 °C).

For some experiments, the surface of the polymer inverse opals was made hydrophilic or hydrophobic to study the effect of interfacial energy of the structure of the MSCs. Hydrophilic cavities were formed by treating the polymer inverse opals with oxygen plasma for 10 s (March GCM-200 Plasmod plasma etcher operating at 50 W). Hydrophobic cavities were generated by treating the polymer inverse opal with a 5 mM octadecyltrichlorosilane (ODTS) hexane solution for 30 s.

**Replication of Polymer Inverse Opals with Mesoporous Silica.** A lyotropic silica precursor mixture was infiltrated within the cavities of the polymer inverse opals by dipping the inverse opal films in the lyotropic mixture for 5 h. The lyotropic mixture contained 10 mM tetraethyl orthosilicate (Aldrich, TEOS), 80 $\mu$M Pluronic F127 triblock copolymer (BASF), 0.1 mM nitric acid (Aldrich), 50 mM ethanol (Fisher Scientific), and 30 mM water. The filled polymer inverse opal composites were removed from the lyotropic mixture solution and subsequently gelled overnight in an oven at ~70 °C. The resulting films were then calcined at 500 °C for 10 h, removing the polyurethane inverse opal template and the triblock copolymer surfactant.

**Instrumentations.** Contact angle measurements were performed on an analyzer (Ramé-Hart NRL CA Goniometer Model 100-00). Morphology studies for the polymer inverse opal templates and the replicated MSC particles were performed using a field emission scanning electron microscope (FE-SEM, Hitachi S-4700) operating with an accelerating voltage of 10 kV. The internal mesostructures of the MSCs were determined by dispersing the MSCs generated after calcination in ethanol using sonication and then depositing the samples on carbon-coated copper TEM grids. Imaging was conducted using a transmission electron microscope (TEM, Philips CM-12) operating at 120 kV.

## Results and Discussion

In this study, polyurethane-based inverse opals, PIO-S, PIO-M, and PIO-L (Figure 1), are utilized as 3D confining environments for the synthesis of MSCs; the cavity diameters (150, 260, and 451 nm) are 10−15% smaller than the diameters (178, 298, and 498 nm) of the respective microspheres used as templates. The cavities are well-ordered with the (111) planes parallel to the substrate; each cavity has multiple interconnecting windows between adjacent cavities. The mean sizes of the interconnecting window are estimated to be 38, 58, and 97 nm for the PIO-S, PIO-M, and PIO-L templates, respectively. These interconnecting windows enable the mesoporous silica precursors to fill all the cavities in the polymer inverse opals. The average number of interconnecting windows per cavity is estimated to be 10.9 (measured from SEM images for PIO-M), 1.1 less than the ideal number of 12 interconnecting windows per cavity. The

(9) Yang, S. M.; Coombs, N.; Ozin, G. A. *Adv. Mater*. **2000**, *12*, 1940.
(10) Jiang, P.; Hwang, K. S.; Mittleman, D. M.; Bertone, J. F.; Colvin, V. L. *J. Am. Chem. Soc*. **1999**, *121*, 11630.
(11) Arriagada, F. J.; Osseo-Asare, K. *J. Colliod Interface Sci*. **1999**, *211*, 210.
(12) Stöber, W.; Fink, A.; Bohn, E. *J. Colloid Interface Sci*. **1968**, *26*, 62.
(13) Jiang, P.; Bertone, J. F.; Hwang, K. S.; Colvin, V. L. *Chem. Mater*. **1999**, *11*, 2123.

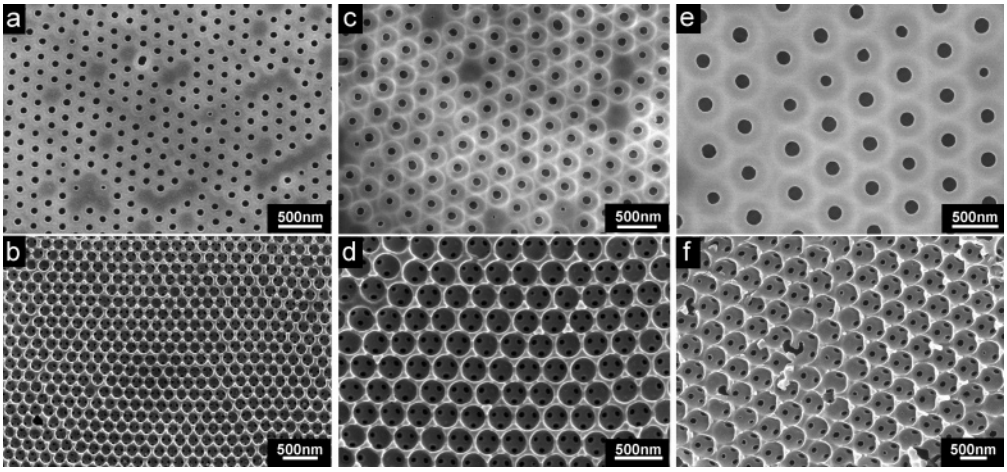


**Figure 1.** SEM images of the polymer inverse opals: (a and b) PIO-S; (c and d) PIO-M; (e and f) PIO-L. Upper row (a, c, and e) are of the polymer−glass interface (after removal of the glass). Lower row (b, d, and f) are cross sections.

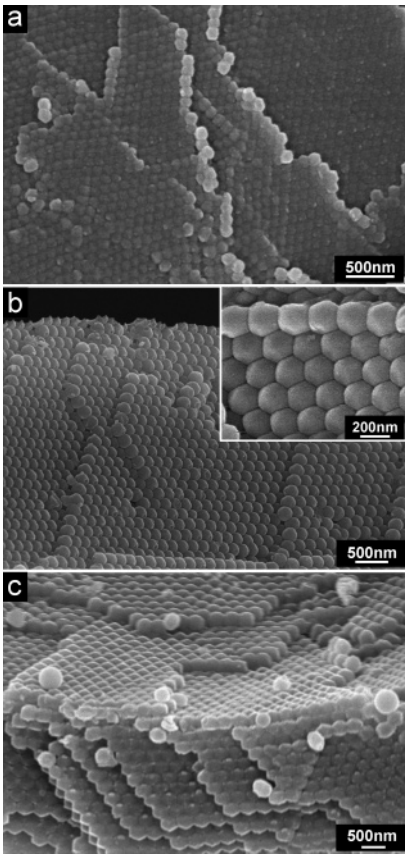


**Figure 2.** SEM images of the MSCs formed in the (a) PIO-S, (b) PIO-M, and (c) PIO-L polymer inverse opals after calcination, but before dispersal.

missing interconnects are probably due to the slight disorder in the silica opal template.

After calcination, the replicated mesoporous silica structure closely resembles the initial silica opal (Figure 2), preserving both the spherical shape and three-dimensional organization as expected, since the double-templating process should return the initial template structure. A well-ordered inverse opal template ideally contains pseudo-rhombohedral dodecahedron cavities;[14] the templated MSCs are shown to have a pseudo-rhombohedral dodecahedron geometry (inset, Figure 2b). The average diameters of the constituent MSCs are found to be 109, 200, and 330 nm for the PIO-S, PIO-M, and PIO-L templates, respectively, ∼26% smaller than the cavity diameters of the polymer inverse opal templates. This volume change is typical for the condensation of the silica precursors during calcination.[15] The MSC precursor fully filled the inverse opal template; after calcination, the structure of the resulting MSCs appeared to be the same through the thickness of the sample. Because the precursor wets the polymer template quite well, and thus completely fills the polymer inverse opal, we expect the structure of the MSCs is not dependent on the thickness of the inverse opal template.

TEM images of the MSCs reveal the expected mesoporous structure (Figures 3 and 4). Interestingly, unlike MSCs formed in the gas phase, which generally contain a single-domain multilayer mesoporous structure,[16] MSCs formed in the polymer inverse opal templates contain multiple mesoporous domains, over all particle diameters studied. A representative MSC containing multiple domains of mesochannel bundles splaying outward in different directions is presented in Figure 4a. Over 70% of the MSCs exhibit this multidomain structure. We strongly suspect the multidomain structure is a direct result of the multiple interconnecting windows between the cavities in the polymer inverse opal template. To confirm the effect of interconnecting windows in the MSC mesostructure, a highly disordered polymer inverse opal was used as a template for MSCs. SEM images (Supporting Information, Figure S2) show that the number of interconnecting windows is reduced to ∼4.2 per cavity; ∼80% of the MSCs formed in the disordered inverse opal template showed a single-domain mesostructure (Figure 4b) rather than the multidomain structure generated by the ordered polymer template.

It is well-known that the lyotropic mesoporous silica precursor mixture cooperatively self-assembles in the bulk with long-range order.[17] If a self-assembled mesophase self-assembles within an ideal windowless spherical nanocavity,

(14) Sun, Z. Q.; Chen, X.; Zhang, J. H.; Chen, Z. M.; Zhang, K.; Yan, X.; Wang, Y. F.; Yu, W. Z.; Yang, B. *Langmuir* **2005**, *21*, 8987.

(15) Feng, P.; Bu, X.; Pine, D. J. *Langmuir* **2000**, *16*, 5304.

(16) Lu, Y.; Fan, H.; Stump, A.; Ward, T. L.; Rieker, T.; Brinker, C. J. *Nature* **1999**, *398*, 223.

(17) Ying, J. Y.; Mehnert, C. P.; Wong, M. S. *Angew. Chem., Int. Ed.* **1999**, *38*, 56.

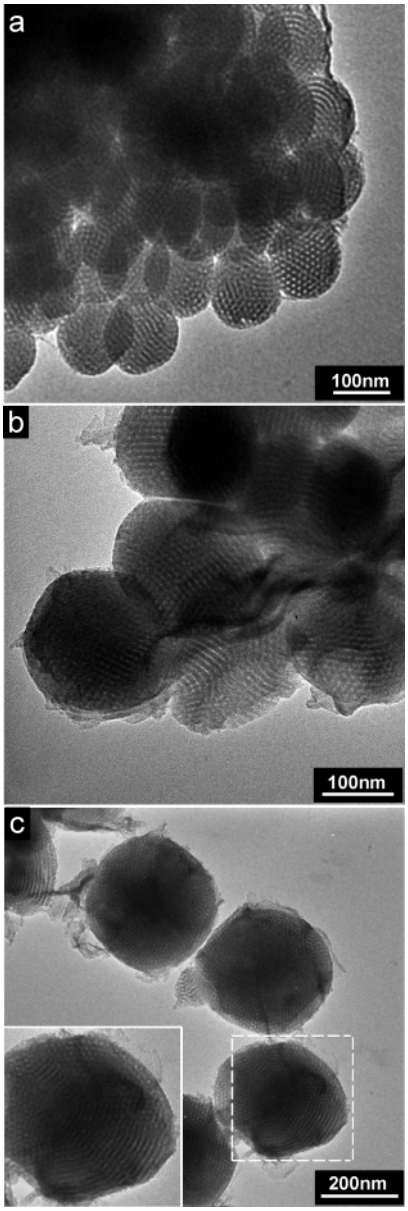


**Figure 3.** TEM images of MSCs formed in the (a) PIO-S, (b) PIO-M, and (c) PIO-L polymer inverse opals.

or in the gas phase, a symmetric mesostructure is expected as a result of the isotropic physical confining force. The polymer inverse opal template, while generally spherical, has spatially organized interconnecting windows, which allows the lyotropic mesoporous silica precursor mixture to communicate between the cavities of the template. It was previously demonstrated that liquid crystal molecules confined in the cavities of an inverse opal communicate through the interconnecting windows, so this result should not be surprising.[18] Here, the communication between the interconnecting windows serves to significantly modify the internal structure of the confined lyotropic mesophase by changing the degree of confinement. Upon close examination, the organization of the bundles of mesochannels in the MSCs appear to mimic the pseudo-rhombohedral dodecahedral

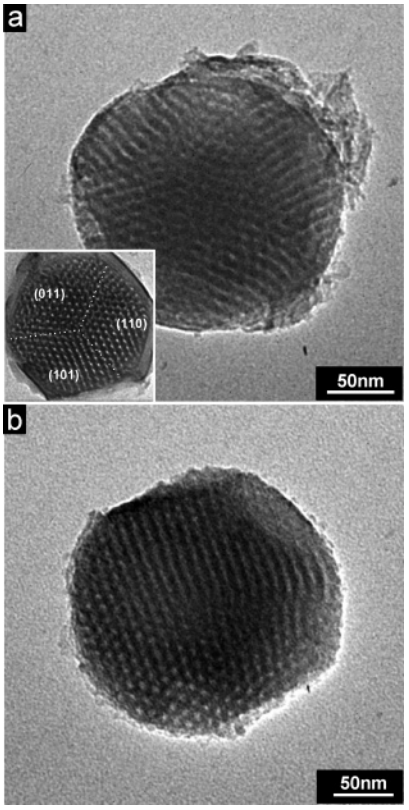


**Figure 4.** TEM images of the templated MSCs formed in (a) ordered and (b) disordered polymer inverse opal templates (PIO-M).

interconnect symmetry found within the polymer opal template (inset of Figure 4a).

In a cavity, interfacial interactions also influence the internal mesostructure of the confined lyotropic mixture. Depending on the organization of the mesophase within the cavity, the mesophase presents very different surface chemistries at the mesophase cavity interface; these different organizations may not be energetically identical. The final organization of the lyotropic mesophase within the cavity is a function of the total energy of the system, including the strain energy of the confined mesophase, interactions through pores between cavities, and the interfacial energy itself; the final structure is determined by a minimization of the total energy of the system. To investigate the effect of interfacial interactions on the final mesostructure of the MSCs, polymer inverse opals with hydrophobic or hydrophilic surfaces were utilized as templates. The as-made polymer inverse opals exhibit intermediate surface energies with water contact angles of $60 \pm 3°$. Once the polyurethane inverse opals are treated with oxygen plasma, the surfaces become very hydrophilic; the water contact angle reduces to $18 \pm 3°$, probably due the formation of peroxide species on the polyurethane surface.[19] The structure of the polymer inverse opal template is not disrupted by the oxygen plasma treatment (Supporting Information, Figure S3). Treatment of the inverse opals with ODTS results in a very hydrophobic surface exhibiting a water contact angle of $105 \pm 3°$.

The hydrophilic polymer inverse opal templates exclusively result in MSCs containing circularly wound concentric

(18) (a) Mach, P.; Wiltzius, P.; Megens, M.; Weitz, D. A.; Lin, K.; Lubensky, T. C.; Yodh, A. G. *Phys. Rev. E* **2002**, *65*, 031720. (b) Mach, P.; Wiltzius, P.; Megens, M.; Weitz, D. A.; Lin, K.; Lubensky, T. C.; Yodh, A. G. *Europhys. Lett.* **2002**, *58*, 679.

(19) Zhang, Y.; Myung, S.-W.; Choi, H.-S.; Kim, I.-H.; Choi, J.-H. *J. Ind. Eng. Chem.* **2002**, *8*, 236.

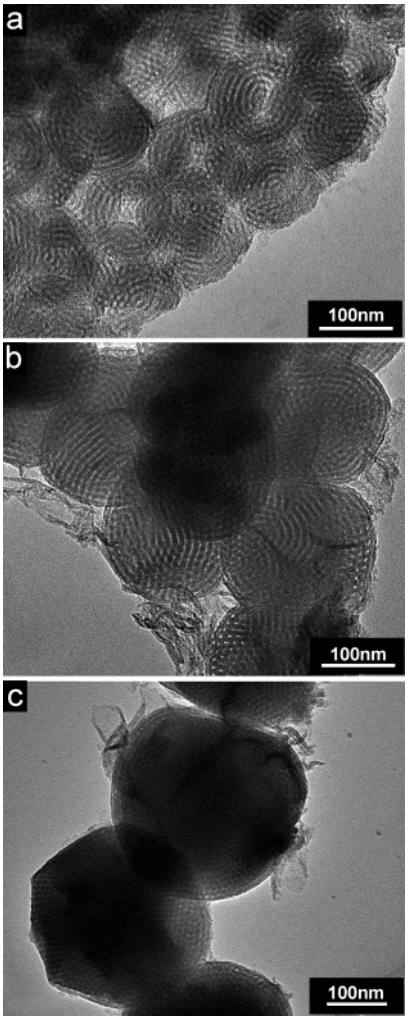


**Figure 5.** TEM images of MSCs formed in hydrophilic polymer inverse opal templates of different cavity diameters. (a) PIO-S, (b) PIO-M, and (c) PIO-L.

mesochannels for all particle diameters studied (Figure 5). The largest MSCs have multiple domains in the center region; however, the circularly wound structure is still observed at the edges of the particles (Figure 5c). In the smaller MSCs, the circularly wound concentric nanochannel assembly propagates to the center of the particle (Figures 5a and 5b). The overall structure of the MSCs formed in the hydrophilic matrix is driven by the fact that it is much more favorable for the hydrophilic polyethylene oxide (PEO)/silica composite block to contact the surface of the polymer cavities than the polypropylene oxide (PPO) block.[20] As a result of the strong interfacial interaction, the mesochannels of the confined mesophase are curved along the internal curvature of the spherical void cavity, even though the inverse opal has multiple interconnecting windows. The interfacial interactions dominate both the supramolecular self-assembly of the lyotropic mesophase, which prefers a hexagonal structure, not a lamellar structure, and any perturbations due to the interconnecting windows.

The interfacial interactions were quite different for the confined mesophase within a hydrophobic inverse opal template. The resulting MSCs contained the expected nearly single-domain mesoporous structure in their centers, as shown in Figure 6. One notable distinction was that the outermost region of the MSC particles was nearly featureless; see inset of Figure 6. The loss of structure at the particle edge appears to originate from unfavorable interactions between the hydrophilic PEO/silica block and the hydrophobic surface. Phase inversion, due to the preference of the PPO block for the hydrophobic polymer surface of the spherical cavity, generally results in the disordered mesostructure at the particle edge.

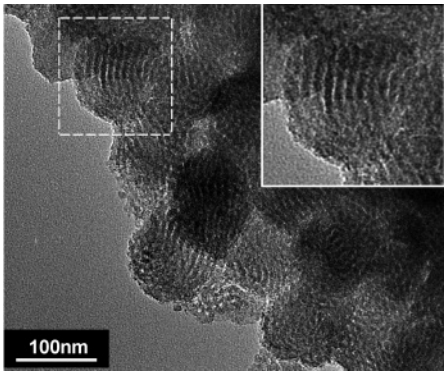


**Figure 6.** TEM image of MSCs formed in a hydrophobic polymer inverse opal template (PIO-S). Inset is a higher magnification image of the selected area.

## Conclusions

Inverse opal polymer templates are used to direct the structure of MSCs and to study the effect of connectivity, surface energies, and diameter on the organization of mesoporous silica. As the surface energy of the polymer template is changed from hydrophilic, to intermediate, and then to hydrophobic, the organization of the mesostructure of the MSCs changes from circularly wound to pseudo-rhombohedral dodecahedral and then to disordered. When the average number of interconnects between cavities is decreased, the pseudo-rhombohedral dodecahedral organization is no longer observed. The ability to define the organization of the mesostructure of MSCs may open applications where transport is important, including supercapacitors, drug delivery, and catalysis.

**Acknowledgment.** This work was supported in part by the Nanoscale Science and Engineering Initiative of the NSF under Awards No. DMR-0117792 and DMI 0404030. Research for this publication was carried out in part in the Center for Microanalysis of Materials, University of Illinois at Urbana−Champaign, which is partially supported by the U.S. Department of Energy under Grants DE-FG02-07ER46453 and DE-FG02-07ER46471. W.-S.C. acknowledges partial fellowship support from a Korea Research Foundation postdoctoral fellowship (M01-2005-000-10012-0).

**Supporting Information Available:** FE-SEM images of the colloidal silica particles of different diameters, ordered and disordered polymer inverse opals, and oxygen plasma-treated polymer inverse opals (PDF). This material is available free of charge via the Internet at http://pubs.acs.org.

CM071642P

(20) (a) Zhao, D.; Huo, Q.; Feng, J.; Chmelka, B. F.; Stucky, G. D. *J. Am. Chem. Soc*. **1998**, *120*, 6024. (b) Ryoo, R.; Ko, C. H.; Kruk, M.; Antochshuk, V.; Jaroniec, M. *J. Phys. Chem. B* **2000**, *104*, 11465.